Electronic Structure Investigation of Highly Compressed Aluminum with *K* Edge Absorption Spectroscopy

A. Benuzzi-Mounaix,[1,*] F. Dorchies,[2] V. Recoules,[3] F. Festa,[1,3] O. Peyrusse,[2] A. Levy,[1] A. Ravasio,[1] T. Hall,[4] M. Koenig,[1] N. Amadou,[1] E. Brambrink,[1] and S. Mazevet[3,5]

[1]*LULI, École Polytechnique, CNRS, CEA, UPMC, route de Saclay, 91128 Palaiseau, France*
[2]*Université de Bordeaux-CNRS-CEA, Centre Lasers Intenses et Applications (CELIA), Talence, F-33405, France*
[3]*CEA, DAM, DIF, F-91297 Arpajon, France*
[4]*Physics Department, University of Essex-Colchester, United Kingdom*
[5]*LUTH, Observatoire de Paris, CNRS, Université Paris Diderot, 5 place Janssen, 92195 Meudon Cedex, France*

(Received 13 May 2011; published 13 October 2011)

The electronic structure evolution of highly compressed aluminum has been investigated using time resolved *K* edge x-ray absorption spectroscopy. A long laser pulse (500 ps, $I_L \approx 8 \times 10^{13}$ W/cm^2) was used to create a uniform shock. A second ps pulse ($I_L \approx 10^{17}$ W/cm^2) generated an ultrashort broadband x-ray source near the Al *K* edge. The main target was designed to probe aluminum at reshocked conditions up to now unexplored (3 times the solid density and temperatures around 8 eV). The hydrodynamical conditions were obtained using rear side visible diagnostics. Data were compared to *ab initio* and dense plasma calculations, indicating potential improvements in either description. This comparison shows that x-ray-absorption near-edge structure measurements provide a unique capability to probe matter at these extreme conditions and severally constrains theoretical approaches currently used.

DOI: 10.1103/PhysRevLett.107.165006 PACS numbers: 52.50.Lp, 32.30.Rj, 52.25.Os, 52.27.Gr

Understanding warm dense matter (WDM), namely, the state of matter lying at the frontier between condensed matter and plasma physics, is of great interest for different fields of physics, such as planetology and inertial confinement fusion [1–5]. This regime of matter is characterized by near or above solid densities and by temperatures up to 100 eV. It is very difficult to calculate its properties. On one hand, the WDM state has moderately to strongly coupled but fluidlike ions, which prohibit the exploitation of long-range order as in solids. On the other hand, expansion techniques commonly used in low density plasma physics where correlations are incorporated perturbatively, are not applicable. In the past ten years, great progress has been made using *ab initio* techniques [6] leading to a refined description of this state of matter over the commonly used average atom models [7].

In parallel, important improvements have been made on the experimental side in both generation and characterization of the WDM state. While pressures below a few Mbar can be studied exhaustively by using static compression methods, investigating high pressures regime ($P>$ a few Mbar) requires dynamic methods such as gas gun, *Z* pinch, or laser driven shocks [8–10]. Standard measurements, including equation of state along the Hugoniot [9] as well as transport properties (e.g., reflectivity and conductivity [11]), only provide indirect information. Nowadays, an effort is underway to develop x-ray diagnostics (e.g., x-ray scattering or radiography [12,13]) to directly access relevant quantities such as density, ionization state, temperature, electronic or ionic structure. In this Letter we present a timed resolved laser compressed Al *K* edge x-ray-absorption near-edge spectroscopy (XANES) study to investigate electronic structure modifications at conditions of density and temperature up to now unexplored.

XANES is a powerful diagnostic since it brings direct information on both valence and core electronic structure, as well as on local atomic order. Consequently, it is suitable to characterize changes of structures and phase transitions. Indeed, it is already widely used in various fields ranging from solid-state physics to chemistry or molecular biology. Only recently it has been applied to the WDM created by laser isochoric proton heating [14], providing direct insights into the dynamic of the solid-to-plasma phase transition around solid density.

Concerning compressed states, the first investigation has been performed on the *K* edge of KCl [15]. Up to now, only work of DaSilva *et al.* [16] and Hall *et al.* [17] investigated *K* edge modification of dense aluminum. These first data were limited by quite low compressions, low temporal resolution ($\approx$ 120 ps in [17]) and a lack of accurate plasma state characterization. The measurements we present here are the first ones obtained at densities up to $3\rho_0$ ($\rho_0 = 2.7$ g/cm^3 is the solid density) with high temporal resolution allowing us to obtain a snapshot of the plasma, at well-defined density and temperature conditions, determined by independent diagnostics. In this way, we were able to study electronic structure at well-controlled thermodynamic conditions.

The experiment has been performed on the LULI2000 laser facility at the Laboratoire pour l'Utilisation des Lasers Intenses (LULI) of the Ecole Polytechnique. This facility has two beams. The first one delivered up to

~150 J at 2ω (532 nm) in 500 ps and was used to generate a shock in the main target. To achieve a uniform compression, the beam was spatially smoothed by an hybrid phase plates (HPP) and focused on a 400 μm diameter flat top focal spot, giving intensities between 1 and 8×10^{13} W/cm^2. The main target was composed of an ablator of plastic (15 μm CH) followed by the material under study (1 μm Al) and a tamped layer (5 μm of diamond). The aluminum thickness is chosen to optimize the contrast of the K edge Al absorption spectrum and the diamond thickness was set to limit the additional induced x-ray absorption. The diamond tamped layer allowed us to maintain Al at high density. The shock is generated in the ablator and then propagates in the Al. When it reaches the Al-diamond interface, the impedance mismatch induces a shock transmitted in the diamond and a reflected shock returning in the Al (see principle on Fig. 1). The Al lies in a reshocked state until the return of the unloading wave that travels back in diamond once the shock breaks out in the void. From hydrodynamic simulations (MULTI code [18]) we know that, for our target, the aluminum stays in extreme conditions during around 200 ps and then unloads.

The second beam delivered 20 J at 2ω in 3.5 ps and it was used to generate an isotropic x-ray source by focusing it on a dysprosium target. Such interaction between a picosecond beam and high Z material creates a spectrally flat emission coming from the M band [19]. The x-ray source duration ($\leq$ 10 ps) is significantly shorter than the 200 ps during which the Al layer is kept compressed. The material was chosen to generate a suitable source around the Al K edge energy (1.5596 keV). This beam was delayed with respect to the main beam, to probe aluminum under reshock conditions. This delay depends on laser intensity and was well predicted by hydrodynamic simulations.

The main diagnostic consisted of two independent spectrometers based on Bragg KAP conical crystals with image plates (IP) detectors. One spectrometer collected the x-ray spectrum transmitted through the main target. The spectrum emitted by the x-ray source was also recorded by the other one (reference). The IP were positioned out of the focal plane of the conical crystals. This setup, already described in [20] provided a spatial resolution of the x-ray absorption along one dimension (transverse to the spectral dispersion axis). We measured a spatial resolution of 35 μm, of the same order of the focal spot of the short pulse beam. The field of view was 700 μm allowing us to record on the same shot the shocked region (which was $\approx$ 400 μm) and the unperturbed region. The spectral resolution (around 2.5 eV) was obtained using a cold Al K edge spectrum measurement. The spectra have been analyzed inferring the absorption from the ratio between the transmitted and the reference signals, using the same protocol as described in [20].

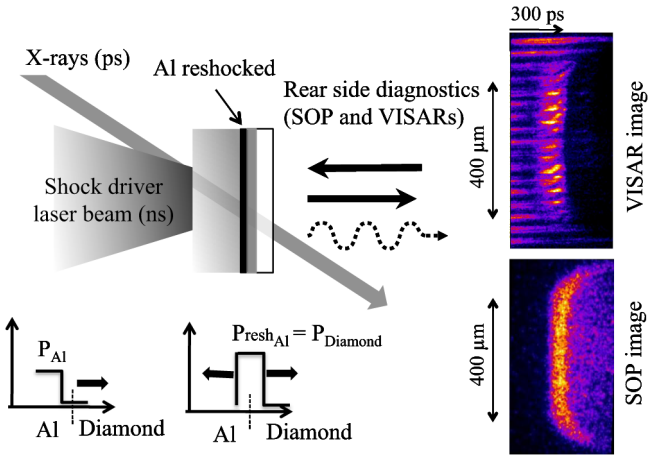

FIG. 1 (color online). Principle of the experiment and VISAR and SOP typical images.

In parallel, a set of two rear side diagnostics was implemented to determine density and temperature of the plasma probed by x-ray spectroscopy. Two VISARs (velocity interferometer system for any reflector) [21] were used to measure the shock velocity in the diamond as the generated shock pressure exceeded the metallization threshold (around 8 Mbar [22]). The self-emission diagnostic was also used to cross-check the mean diamond shock velocity. Typical shock velocities ranged between 24 and 35 km/s, depending on the laser intensity. We coupled these data with hydrodynamic simulations and adjusted the numerical laser intensity to reproduce the experimental data. This allowed us to evaluate the density ρ and the temperature T of the probed aluminum. In the simulations we used 3717 and 7830 SESAME EOS tables for Al and C, respectively. This procedure has been previously established as a valid tool to describe the time evolution of shock compressed targets [12]. The spatial uniformity (along the shock direction) of the compressed aluminum layer was highly satisfying (see Fig. 2 on the right).

All the probed conditions are presented in Fig. 2 in the plane (ρ, T). Figure 2 also shows the principal Hugoniot and reshocked states of aluminum, as given by the 3717 SESAME library [23] equation of state. Depending on the quality of the shot, the precision on the shock velocity varied between $\pm$4% and $\pm$7%. This induced an uncertainty on the numerical laser intensity used to reproduce the measured shock velocity. This leaded to an error on the temperature and density (obtained from the simulations) that did not exceed $\pm$20% and $\pm$8%, respectively. The uncertainty on the timing probe has been also included in the plotted error bars.

Three sets of measurements are reported in Fig. 2. Data corresponding to short delays ($\approx$ 100 ps) between the x-ray source and the main beam give us information on Al conditions before the compression. As it can be observed (orange round data), the aluminum is slightly, but negligibly preheated ($T \leq 0.3$ eV). With delays of

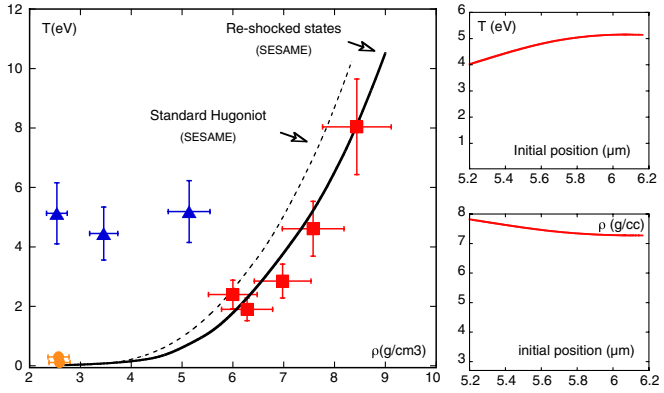

FIG. 2 (color online). On the left, ρ and T probed aluminum conditions inferred by the shock velocity VISAR/SOP data coupled with the hydrodynamic simulations. On the right, a typical ρ and T spatial profile along the shock direction of 1 μm probed Al, given by the Lagrangian code. Different colors refer to different probe times. Orange circles: early time (before shock). Red squared: intermediate times (reshocked conditions). Blue triangles: late times (unloading conditions).

about 500 ps, depending on the laser intensity, we reached conditions well off the principal Hugoniot (red squared data). By setting a larger delay between the two beams ($\approx$ 900 ps) we investigated the unloading conditions accessing a wider region of the Al phase diagram (blue triangles data). This broad set of conditions allowed us to analyze the modifications of the electronic structure and 1s level along the reshocked states and separates the influence of temperature and density on the XANES spectrum.

In Fig. 3(a), we show some experimental spectra representing the X-ray absorption, corresponding to preheated and reshocked data (see Fig. 2). We can observe a spectrum at standard conditions ($\rho = \rho_0$ and $T = 0.025$ eV) with typical XANES structures and a spectrum at $\rho \approx \rho_0$ and $T \approx 0.3$ eV with a smoothing of these structures due to the loss of ion-ion order. This result is consistent with results previously obtained by isochoric heating [14]. Concerning the other spectra, corresponding to reshock conditions, we also observe strong perturbations of the K edge as the density and temperature increase. On the theoretical side, an important work has been done in parallel with the experiment, to calculate a set of XANES spectra in a range of densities between 2.7–8.1 g/cc and temperature up to 7 eV (e.g., a series of spectra along isotherms at 5 and 2.5 eV and along isochors at 8.1 g/cc have been calculated). On Figs. 3(b) and 3(c), we show spectra obtained using two different theoretical approaches at (ρ, T) conditions close to the experimental ones. This qualitative comparison is relevant since these conditions are inside the experimental error bars.

The first calculation is based on *ab initio* approach described in details in Refs. [24,25]. The second one involves a finite-temperature neutral pseudoatom concept of dense matter coupled to a real-space finite-difference computation of XANES structures and is described in Ref. [26].

The overall modifications of the experimental spectra are well reproduced by both models. In particular, the loss of XANES structure as temperature rises and the general trend in the K edge modification are well reproduced. In more details, we note that *ab initio* calculations show a better agreement concerning the evolution of the K edge and XANES structures. Indeed it has been shown that this type of calculation is well adapted to accurately describe the ionic structure, correlations for WDM conditions and particularly the transition between solid, liquid, and plasma states [6,27].

The high quality of our data allowed us to go a step further and quantify the variation of the XANES spectra. To overcome the difficulty in defining a threshold for the K edge, we fit the edge using a function $f(E) = a^*(E\text{-}E_k)$, where a is the slope and E_k defines the K edge position. The shift is then given as E_k-E_{k0}, where E_{k0} is the K edge position at Al standard conditions [see Fig. 3(a)].

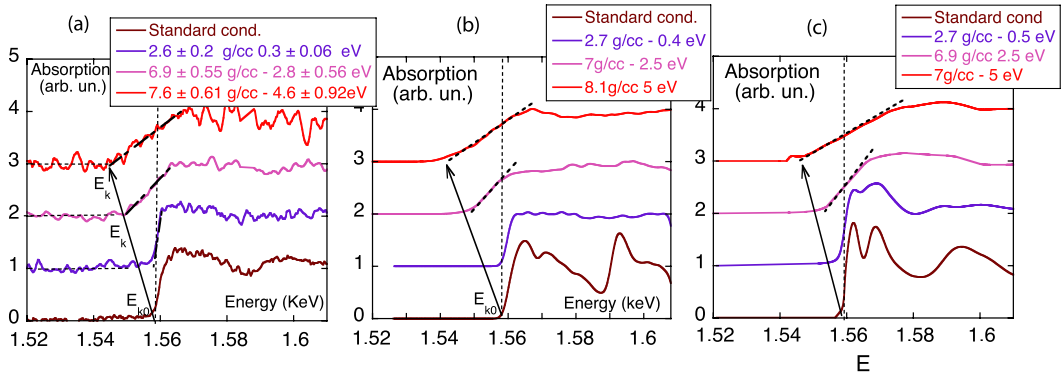

FIG. 3 (color online). (a) Some experimental K edge XANES spectra for reshocked conditions (deduced by rear side diagnostics—see Fig. 2). The "standard cond." corresponds to a shot without the ns shock beam (solid density and room temperature); (b), (c) Calculated K edge XANES spectra: (b) *ab initio* data (a constant shift of 90 eV was applied to all the *ab initio* calculations Ref. [25]) and (c) dense plasma model data. All the spectra are normalized to the x-ray absorption value far above the K edge.

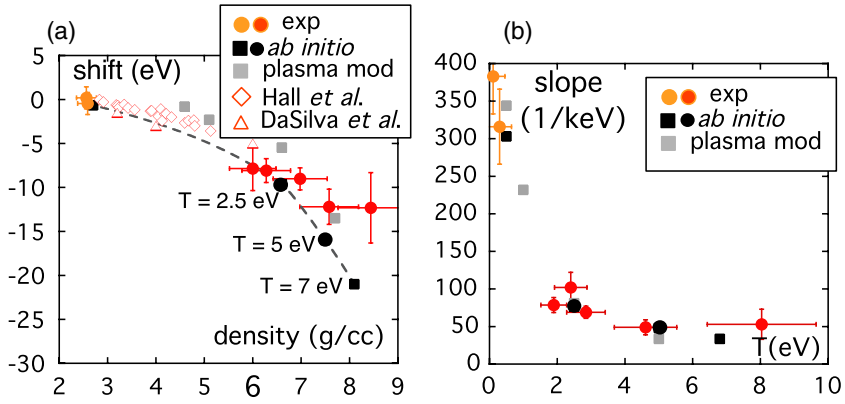

FIG. 4 (color online). (a) K edge shifts (b) and slope along reshocked conditions (see Fig. 2). The black circles *ab initio* points were deduced by performing a fit on the *ab initio* 2.5 and 5 eV isotherms (e.g., see Fig. 5).

Figure 4 shows the results of this analysis when applied to both the theoretical and experimental spectra. We also show previous measurements to highlight the important role of our data that lie in a region up to now never investigated.

We found in previous works [24–26] that the slope of the K edge depends mainly on temperature. The decrease of the slope (i.e., the increasing of broadening) is due to the thermal depopulation of the energy levels below the Fermi level. Figure 4(b) indicates that the variation of the experimental slopes is in good agreement with both models.

The shift, as defined here, is driven by two contributions: one coming from temperature via the decreasing of the slope and one from density, via the competing effect of the increase of both the Fermi energy and the $1s$ orbital energy. The measured shifts [Fig. 4(a)] are towards lower energies, as expected [24,26]. At extreme conditions, they are slightly less important than predicted by *ab initio* calculations. The good agreement found above for the slope suggests that the difference comes from the density contribution. Thanks to the broad investigation of the phase diagram, we were able to isolate the density effect by selecting measurements at a constant temperature of around 5 eV (blue triangles in Fig. 2).

Figure 5 indicates that, when density goes from ρ_0 to $3\rho_0$, the experimental shift increase remains moderate (it goes from ≈ -7.5 eV to ≈ -12 eV). For the same conditions, the *ab initio* data overestimate the redshift by ≈ 4 eV. This overestimation is satisfyingly consistent with what we found at the highest densities along the reshocked Hugoniot [Fig. 4(a)]. Since there is a consensus on the dependence of the Fermi energy on density [24,26], this disagreement should be attributed to the $1s$ level energy shift. Indeed the two theoretical approaches differ significantly on this point [24,26]. The $1s$ level shift is affected both by the neighboring atoms and by the description of the excited atom. Both of the effects have been studied within the model of [26] in an attempt to go beyond the one-electron picture approximation. This study indicates that these effects need to be better described in the *ab initio* calculations by relaxing the core orbital to go beyond the frozen core approximation and improve on the impurity model [25]. We further note that when performing a finite temperature DFT calculation, this cannot be accessed directly by using an all electron pseudopotential for the absorbing atom if ones want to use the impurity model where the $1s$ orbital is half occupied.

In summary, we studied the aluminum electronic structure at well controlled (ρ, T) conditions in a unexplored and extreme region of the phase diagram. The comparison with two theoretical models provide an overall satisfying agreement with the data but it is found that both models need improvements to describe in details the variation of the XANES spectra and the K edge shift. This work shows that by directly accessing the variation of the electronic structure, time resolved K edge measurements of dense plasma provide a stringent test to theoretical models. In the current case this allows us to point to the need to go beyond the frozen core approximation in the *ab initio* description.

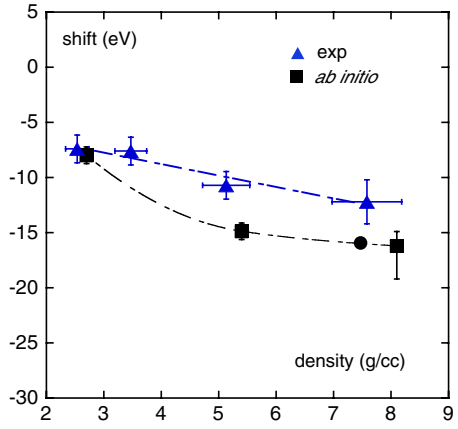

FIG. 5 (color online). Comparison between experimental and *ab initio* calculated K edge shift at $T \approx 5$ eV, as function of ρ. The black circle corresponds to the point deduced from the fit and shown in Fig. 4(a).

We wish to acknowledge for useful discussions T. Vinci as well as the support of the GENCI program for providing computational time under the program GEN6046 and GEN6454.

*alessandra.benuzzi-mounaix@polytechnique.fr

[1] G. Collins *et al.*, Science **281**, 1178 (1998).
[2] M. Knudson *et al.*, Phys. Rev. Lett. **87**, 225501 (2001).
[3] M. Koenig *et al.*, Appl. Phys. Lett. **72**, 1033 (1998).
[4] G. Huser *et al.*, Phys. Plasmas **12**, 060701 (2005).
[5] J. Eggert *et al.*, Phys. Rev. Lett. **100**, 124503 (2008).
[6] L. A. Collins *et al.*, Phys. Rev. B **63**, 184110 (2001).
[7] D. A. Liberman, Phys. Rev. B **20**, 4981 (1979).
[8] J. H. Nguyen and N. C. Holmes, Nature (London) **427**, 339 (2004).
[9] M. Koenig *et al.*, Phys. Rev. Lett. **74**, 2260 (1995).
[10] M. Knudson and M. P. Desjarlais, Phys. Rev. Lett. **103**, 225501 (2009).
[11] P. M. Celliers *et al.*, Phys. Plasmas **11**, L41 (2004).
[12] A. Ravasio *et al.*, Phys. Rev. Lett. **99**, 135006 (2007).
[13] S. Glenzer *et al.*, Phys. Rev. Lett. **98**, 065002 (2007).
[14] A. Mancic *et al.*, Phys. Rev. Lett. **104**, 035002 (2010).
[15] D. Bradley *et al.*, Phys. Rev. Lett. **59**, 2995 (1987).
[16] L. DaSilva *et al.*, Phys. Rev. Lett. **62**, 1623 (1989).
[17] T. A. Hall *et al.*, Europhys. Lett. **41**, 495 (1998).
[18] R. Ramis *et al.*, Comput. Phys. Commun. **49**, 475 (1988).
[19] M. Harmand *et al.*, Phys. Plasmas **16**, 063301 (2009).
[20] A. Levy *et al.*, Rev. Sci. Instrum. **81**, 063107 (2010).
[21] L. M. Barker and Hollenbach, J. Appl. Phys. **43**, 4669 (1972).
[22] D. Bradley *et al.*, Phys. Rev. Lett. **93**, 195506 (2004).
[23] SESAME, Report No. LA-UR-92-3407, 1992.
[24] S. Mazevet and G. Zerah, Phys. Rev. Lett. **101**, 155001 (2008).
[25] V. Recoules and S. Mazevet, Phys. Rev. B **80**, 64 110 (2009).
[26] O. Peyrusse, High Energy Density Phys. **6**, 357 (2010).
[27] M. P. Desjarlais *et al.*, Phys. Rev. E **66**, 025401(R) (2002).